THE JOURNAL OF BIOLOGICAL CHEMISTRY
Vol. 280, No. 23, Issue of June 10, pp. 22258–22269, 2005
Printed in U.S.A.

The X-ray Structure of a Hemipteran Ecdysone Receptor Ligand-binding Domain

COMPARISON WITH A LEPIDOPTERAN ECDYSONE RECEPTOR LIGAND-BINDING DOMAIN AND IMPLICATIONS FOR INSECTICIDE DESIGN*

Received for publication, January 19, 2005, and in revised form, March 22, 2005
Published, JBC Papers in Press, April 4, 2005, DOI 10.1074/jbc.M500661200

Jennifer A. Carmichael‡, Michael C. Lawrence‡§, Lloyd D. Graham¶, Patricia A. Pilling‡, V. Chandana Epa‡, Leonie Noyce¶, George Lovrecz‡, David A. Winkler‖, Anna Pawlak-Skrzecz¶, Ruth E. Eaton¶, Garry N. Hannan¶, and Ronald J. Hill¶**

From ‡CSIRO Health Sciences and Nutrition, 343 Royal Parade, Parkville, Victoria 3052, Australia, ¶Commonwealth Scientific and Industrial Organization, Molecular Science, P. O. Box 184, North Ryde, New South Wales 1670, Australia, and ‖Commonwealth Scientific and Industrial Organization, Molecular Science, Private Bag 10, Clayton South MDC, Victoria 3169, Australia

The ecdysone receptor is a hormone-dependent transcription factor that plays a central role in regulating the expression of vast networks of genes during development and reproduction in the phylum Arthropoda. The functional receptor is a heterodimer of the two nuclear receptor proteins ecdysone receptor (EcR) and ultraspiracle protein. The receptor is the target of the environmentally friendly bisacylhydrazine insecticides, which are effective against Lepidoptera but not against Hemiptera or several other insect orders. Here we present evidence indicating that much of the selectivity of the bisacylhydrazine insecticides can be studied at the level of their binding to purified ecdysone receptor ligand-binding domain (LBD) heterodimers. We report the crystal structure of the ecdysone receptor LBD heterodimer of the hemipteran *Bemisia tabaci* (Bt, sweet potato whitefly) in complex with the ecdysone analogue ponasterone A. Although comparison with the corresponding known LBD structure from the lepidopteran *Heliothis virescens* (Hv) ecdysone receptor revealed the overall mode of ponasterone A binding to be very similar in the two cases, we observed that the BtEcR ecdysteroid-binding pocket is structured differently to that of HvEcR in those parts that are not in contact with ponasterone A. We suggest that these differences in the ligand-binding pocket may provide a molecular basis for the taxonomic order selectivity of bisacylhydrazine insecticides.

The nuclear receptor (NR)[1] family of proteins plays a crucial role in the regulation of transcription, and its members include the receptors for steroid hormones, vitamins, thyroid hormones, and bile acids (1). The human genome contains about 48 members of this family, and these have been studied extensively as therapeutic targets (2). The Arthropoda display a more limited suite of NRs (3) about 21 of which occur in *Drosophila melanogaster*. Among these is the receptor for the major arthropod steroid hormone, 20-hydroxyecdysone, which is involved in the regulation of insect molting, metamorphosis, and reproduction (4–9). The receptor is absent from mammals and is thus potentially useful as a safe insecticide target. Indeed members of the bisacylhydrazine family exert their insecticidal activity by binding to the ecdysone receptor and exhibit remarkable taxonomic order selectivity (10, 11). These compounds act selectively on the Lepidoptera and certain Coleoptera (10) but are ineffective against insects of the hemipteran order and therefore cannot be used to control certain insect pests. A study (12) of two hemipteran insect predators (*Geocoris punctipes* and *Orius insidiosus*) showed that these beneficial (predatory) hemipterans are relatively insensitive to the bisacylhydrazine tebufenozide, whereas lepidopteran insect pests are susceptible. An improved understanding of variation in the structure of the ligand-binding pockets of ecdysone receptors and the basis of the specificity of these compounds at the atomic level of detail of their interaction with the receptor may aid the discovery of novel insecticidal ligands with new defined spectra of activity.

Structural studies across the NR family have shown that its members share a common modular structure (13–15) with the most highly conserved C and E domains being associated with DNA binding and ligand binding, respectively. The NR ligand-binding domains (LBDs) share a fold characterized by 12 α-helices (H1–H12) arranged as an antiparallel three-layer sandwich with a β-hairpin in the loop between helices H5 and H6. The ligand-binding pocket lies in a topologically conserved region within the canonical α-helical sandwich and is formed by side chains of residues from helices H3, H5, H7, H11, and H12 and the β-hairpin. The ecdysone receptor itself is a heterodimer of two partner nuclear receptor proteins, EcR (which contains the binding pocket for ecdysteroids) and the ultraspiracle protein (USP), a homologue of the retinoid X receptor (RXR) (5–7).

Three-dimensional structures of the lepidopteran *Heliothis*

* The costs of publication of this article were defrayed in part by the payment of page charges. This article must therefore be hereby marked "*advertisement*" in accordance with 18 U.S.C. Section 1734 solely to indicate this fact.

The atomic coordinates and structure factors (code 1Z5X) have been deposited in the Protein Data Bank, Research Collaboratory for Structural Bioinformatics, Rutgers University, New Brunswick, NJ (http://www.rcsb.org/).

§ To whom correspondence regarding structure information may be addressed. Tel.: 61-3-9662-7100; Fax: 61-3-9662-7347; E-mail: mike.lawrence@csiro.au.

** To whom correspondence regarding biology information may be addressed. Tel.: 61-2-9490-5076; Fax: 61-2-9490-5005; E-mail: ron.hill@csiro.au.

[1] The abbreviations used are: NR, nuclear receptor; EcR, ecdysone receptor; LBD, ligand-binding domain; Dm, *D. melanogaster*; USP, ultraspiracle protein; RXR, retinoid X receptor; Hv, *H. virescens*; Bt, *B. tabaci*; PonA, ponasterone A (25-deoxy-20-hydroxyecdysone); LXRβ, liver X receptor-β; FXR, farsenoid X-activated receptor; RAR, retinoic acid receptor.

virescens ecdysone receptor LBD heterodimer (HvEcR/HvUSP-LBD) have been described recently (16) in complex with the ecdysteroid ponasterone A (PonA, 25-deoxy-20-hydroxyecdysone) and with the non-steroidal bisacylhydrazine agonist BYI06830. PonA is identical to the native ligand (20-hydroxyecdysone) except that it lacks a hydroxyl group at the C-25 position so its mode of binding to the EcR-LBD likely mimics that of 20-hydroxyecdysone. The BYI06830-bound structure demonstrates that the ecdysteroid-binding pocket of the HvEcR-LBD distorts to allow the binding of this compound. In particular, accommodation of the 1,4-dioxan ring of the compound requires the opening up of a cleft between helices H7 and H10 at one end of the pocket as well as side chain and backbone rearrangements of residues at the opposite end of the pocket to fill in the otherwise unoccupied volume of the ecdysteroid-binding pocket. This mode of binding was entirely unanticipated and demonstrated that the ecdysteroid-binding pocket of this EcR-LBD has a level of flexibility not normally seen in nuclear receptor LBDs. It was proposed (16) that the relative specificity of BYI06830 for the lepidopteran EcR relates to amino acid variation at a site corresponding to Val-384 in HvEcR that is substituted by methionine in other insect orders (including the hemipterans). The presence of a larger methionine side chain at this position in the latter orders was argued to have the potential to interfere either directly or indirectly with the binding of bisacylhydrazine compounds such as BYI06830. The structure of HvUSP-LBD in its heterodimeric form is essentially identical to that of the HvUSP-LBD monomer (17, 18) and that of the *D. melanogaster* USP-LBD monomer (17) (DmUSP-LBD). In all of these USP-LBD structures, lipid occupies volume that coincides in part with that of the canonical NR-LBD binding pocket with the lipid head group protruding from the protein surface.

We report here that much of the selectivity of the bisacylhydrazine insecticides can be observed at the level of binding to purified recombinant LBD heterodimers of the ecdysone receptor derived via a baculovirus expression system. In this regard our results showed that the bisacylhydrazine compound tebufenozide has a much lower affinity for the ecdysone receptor of the hemipteran insect *Bemisia tabaci* (sweet potato whitefly) than it does for the corresponding receptor of the lepidopteran insect *Helicoverpa armigera*, thereby reflecting results obtained *in vivo* and in the field (10–12).

We also determined the three-dimensional structure of the ecdysone receptor LBD heterodimer of *B. tabaci* in complex with PonA. Comparison of our structure with those of the *H. virescens* ecdysone receptor LBD heterodimer revealed that regions of the ligand-binding pocket not in contact with the hormone vary significantly between the two structures. We tentatively propose that these differences at the atomic level of detail underlie the selectivity of the bisacylhydrazine insecticides. This first three-dimensional structure of a hemipteran ecdysone receptor LBD heterodimer is of potential value for the molecular design of new insecticides with selective toxicity for plant-sucking bugs.

MATERIALS AND METHODS

Cloning, Expression, and Purification of Ecdysone Receptor LBDs—The cloning, baculovirus-driven expression, and purification of the recombinant ecdysone receptor LBD heterodimer and the corresponding heterodimers from the cloned ecdysone receptors of *Lucilia cuprina* (Diptera), *Myzus persicae* (Hemiptera), and *H. armigera* (Lepidoptera) will be described in detail elsewhere but are in part based on the methods used for the *L. cuprina* receptor (19, 20). In the case of the *B. tabaci* receptor, cDNAs encoding BtEcR-LBD and BtUSP-LBD were screened out of a high quality *B. tabaci* cDNA library in Lambda ZapII (Stratagene) using the corresponding homologous C domain probes PCR-amplified from *B. tabaci* genomic DNA. Segments encoding the D and E domains of BtEcR (residues from Pro-120 to Ser-416) and BtUSP (residues Lys-246 to Ser-496) were subcloned into pFastBac Dual (Invitrogen) with a hexahistidine-encoding tag incorporated N-terminal to the BtEcR segment and a FLAG-encoding tag N-terminal to the BtUSP segment. Analogous constructs were prepared for expression of the ecdysone receptor LBD heterodimers from the other insects. The segments were transposed into a bacmid for baculovirus construction and expression in Hi-5 insect cells. Expressed recombinant ecdysteroid-binding protein was saturated with PonA (a gift from Denis Horn) and purified in the presence of 2-mercaptoethanol and PonA by nickel-nitrilotriacetic acid-agarose affinity chromatography followed by high performance gel filtration (with >60% yield for each step). Polyacrylamide gel electrophoresis of freshly purified ecdysone receptor LBD heterodimers showed bands corresponding to the full-length recombinant polypeptides.

TABLE I
X-ray data collection and crystallographic refinement statistics

No. of frames	302
Oscillation increment (°)	0.5
No. of measurements	191,046
No. of reflections	16,756
Measurement multiplicity	11.4 (10.5)[a]
Resolution range (Å)	30.0–3.07
Completeness (%)	99.9 (100.0)
$I/\sigma(I)$	19.3 (5.6)
R_{sym}[b]	0.13 (0.51)
R_{cryst}[c]	0.203
R_{free} (5% of total reflections)	0.275
r.m.s.d.[d] from ideality	
Bond lengths (Å)	0.012
Bond angles (°)	1.6
No. of protein atoms	3,475
No. of ligand + solvent atoms	53

[a] Numbers in parentheses refer to statistics in the highest resolution shell (3.11–3.07 Å).
[b] $R_{sym} = \Sigma_h\Sigma_i|I_{ih} - \langle I_h\rangle|/\Sigma_h\Sigma_i|I_{ih}|$.
[c] $R_{cryst} = \Sigma_h|F_h^{obs} - kF_h^{calc}|/\Sigma_h|F_h^{obs}|$.
[d] Root mean square deviation.

Competitive Inhibition of Ligand Binding—The binding of 1.3 nM [^{3}H]ponasterone A (PerkinElmer Life Sciences) to purified recombinant receptor LBD heterodimer was measured in the presence of different concentrations of non-radioactive bisacylhydrazine insecticide RH5992 (tebufenozide, *N-tert*-butyl-*N*′-(4-ethylbenzoyl)-3,5-dimethylbenzohydrazide). After 4 h at 21 °C, bound tracer was measured using a modification of a standard method (4) and expressed relative to that in RH5992-free assays. The resulting activity values were corrected for any effects of the dimethyl sulfoxide used as solvent for RH5992 (<1% (v/v) final concentration). IC_{50} values were obtained from smooth curves drawn through the data points, and from these K_i values were calculated using the Cheng-Prusoff equation (21).

Crystallization—Crystals of the PonA-complexed *B. tabaci* ecdysone receptor LBD were grown by vapor diffusion (22) using as well solution 1.0 M $NH_4H_2PO_4$, 4.5% (w/v) D-(+)-trehalose dihydrate, 10 mM dithiothreitol in 0.1 M NaHEPES buffer (pH 7.5). Hanging drops contained 1 μl of well solution plus 1 μl of protein solution at 40 mg/ml in 0.23 M NaCl, 10% (v/v) glycerol, 10 mM dithiothreitol, 3 mM NaN_3, 3 μM PonA, and 50 mM Tris/HCl buffer (pH 7.5). Crystallization trays were maintained at room temperature in a nitrogen environment. Crystals appeared after 3 months and had a maximum dimension of 0.5 mm. SDS-PAGE analysis of crystals and of stored protein revealed polypeptides of somewhat lower molecular weight than expected, presumably the result of progressive proteolysis. N-terminal sequencing of major bands extracted from the gel (data not shown) succeeded in identifying one band as corresponding to a sequence starting at BtUSP residue Leu-285, *i.e.* midway through helix H1.

Diffraction Data Collection and Processing—A single crystal of the PonA-complexed *B. tabaci* ecdysone receptor LBD was transferred to a solution identical in composition to the well solution but with 30% (v/v) glycerol incorporated as cryoprotectant. Diffraction data were then collected at −160 °C using an R-AXIS IV image plate detector (Rigaku-MSC) mounted on a rotating anode M18XHF-SRA x-ray generator (Siemens). All data processing was conducted with HKL (23). The relevant statistics are shown in Table I. The crystal belonged to space group $P4_32_12$ with $a = b = 143.01$ Å, $c = 84.01$ Å and diffracted to ~3.0-Å resolution.

Structure Determination and Refinement—The initial structure was determined using molecular replacement. As this task was performed prior to the structure of the *H. virescens* ecdysone receptor LBD becom-

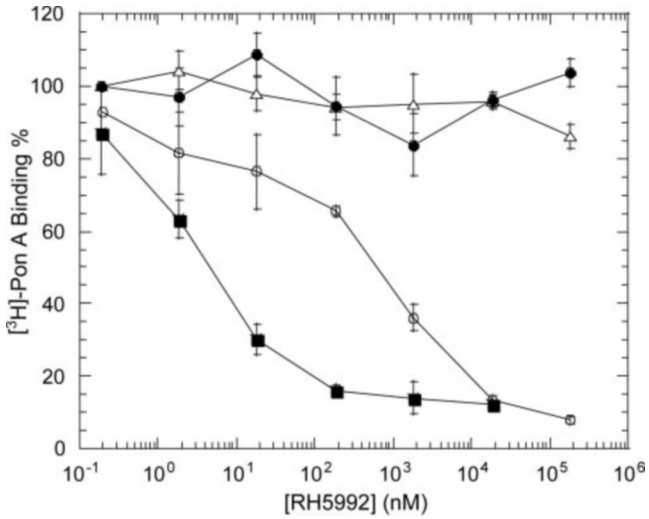

FIG. 1. **Competitive inhibition of [^{3}H]PonA binding to recombinant ecdysone receptor LBD heterodimers by the bisacylhydrazine RH5992.** Receptor LBDs used are the dipteran *L. cuprina* (○), the hemipterans *M. persicae* (△) and *B. tabaci* (●), and the lepidopteran *H. armigera* (■). Data are means ± S.E. with $n = 4$ (except for *H. armigera* where $n = 2$).

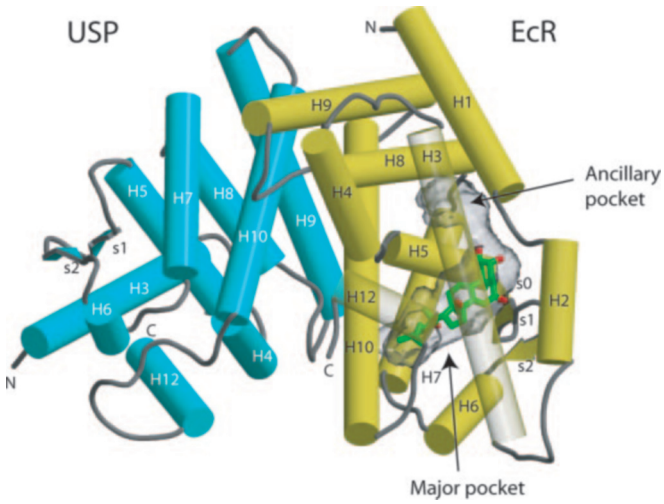

FIG. 2. **Schematic diagram of the structure of the *B. tabaci* ecdysone receptor LBD heterodimer showing the ecdysteroid-binding pocket.** BtEcR-LBD is shown in *yellow*, and BtUSP-LBD is shown in *cyan*. Individual helices are shown as *cylinders*, and individual β-strands are shown as *arrows*. The observed termini of each LBD are labeled. PonA is shown in *green* with oxygen atoms in *red*. Helices H3 and H12 of BtEcR-LBD are rendered *transparent* to enable viewing of the PonA moiety. The surface of the binding pocket is shown in *transparent gray*. The figure was produced using MOLSCRIPT (54), CONSCRIPT (55), and RASTER-3D (56).

ing available, molecular replacement used as search object a homology model of the *B. tabaci* ecdysone receptor LBD built from the structure of the RAR/RXR-LBD heterodimer (24). Molecular replacement was performed using the program MOLREP (25) within CCP4 (26). Iterative crystallographic refinement and model building were conducted using CNS (27) and O (28), respectively, and yielded a model encompassing residues Pro-179 to Val-415 of BtEcR and Val-300 to Ser-492 of BtUSP (*i.e.* encompassing helices H1–H12 of the BtEcR-LBD and helices H3–H12 of the BtUSP-LBD). The ligand PonA was clearly visible within the BtEcR-LBD, and the orientation and location of the four-member ring complex and the alkyl chain could be modeled unambiguously. Also included in the model were three phosphate ions, presumably arising from the solution used for crystallization of the heterodimer. The final crystallographic refinement statistics (Table I) are acceptable given the resolution limit of the data. PROCHECK (29) revealed that only two residues (BtEcR Ile-180 and BtUSP Thr-363) lay in the disallowed regions of the Ramachandran plot. Atomic coordinates have been deposited in the Protein Data Bank under code 1Z5X.

Structural Analysis—Protein cavity analysis and cavity volume computation were conducted with VOIDOO (30) and O (31) using a 1.4-Å probe radius unless otherwise stated. A 1.2-Å probe radius was used to detect features not detected by the larger probe radius cavity calculations (32). Particular care was taken in detecting cavities connected to the surface using the "atom fattening" van der Waals growth factor parameter within VOIDOO. Protein structural overlays were computed using LSQMAN (33) or O (31), molecular surface areas were computed using the program MS (33), surface hydrophobicity analysis was carried out using AREAIMOL (26), atom contact analysis was done using CNS (27), and hydrogen bond calculations were carried out using HBPLUS (34).

RESULTS

Binding of the RH5992 to Cloned Ecdysone Receptor LBDs—Fig. 1 shows a direct comparison of the ability of the bisacylhydrazine insecticide RH5992 to compete with tritiated PonA *in vitro* for binding to the purified recombinant ecdysone receptor LBD heterodimers from lepidopteran, dipteran, and hemipteran ecdysone receptors. The competition curves showed that the compound RH5992 has highest affinity for the heterodimer of the lepidopteran insect *H. armigera* ($K_i \sim 4$ nM), intermediate affinity for the dipteran insect *L. cuprina* ($K_i \sim 240$ nM), and minimal affinity for the hemipteran insects *B. tabaci* ($K_i \geq 480$ μM) and *M. persicae* ($K_i \geq 140$ μM). The K_i values we obtained with the recombinant *L. cuprina* and *H. armigera* heterodimers are close to the dissociation constants reported for RH5992 with cellular extracts from other dipteran (192 nM) and lepidopteran insects (3–13 nM), respectively (10). Thus the ranking of the affinities we obtained for each taxonomic order mimics that observed *in vivo* (10, 11).

Tertiary Structure of the B. tabaci Ecdysone Receptor LBD Heterodimer—Our atomic model of the *B. tabaci* ecdysone receptor LBD heterodimer encompasses residues Pro-179 to Val-415 of the BtEcR polypeptide and residues Val-300 to Ser-492 of the BtUSP polypeptide (Figs. 2 and 3) and has been crystallographically refined to a resolution of 3.1 Å with an R-factor of 0.203 ($R_{free} = 0.275$ (35)). Both the BtEcR-LBD and the BtUSP-LBD have the anticipated canonical NR fold. The β-sheet of the BtEcR-LBD is, like that of HvEcR-LBD, elaborated by a short, additional β-strand (denoted s0) N-terminal to the first canonical β-strand. Helix H12 of BtEcR-LBD is in the canonical agonist conformation (15), and PonA is bound in a totally enclosed pocket within the α-helical sandwich of the BtEcR-LBD. The BtEcR-LBD pocket exhibits a J-shaped architecture (Fig. 4) composed of an elongated portion containing the ligand PonA (the "major pocket") and an additional curved portion (which we term the "ancillary pocket"). The average temperature factor for the PonA atoms is 34 Å^2 compared with 42 Å^2 for the 19 BtEcR atoms within 3.5 Å of the ligand, implying that PonA is well ordered within the protein environment. The interactions between BtEcR-LBD and PonA include seven potential hydrogen bonds as well as a large number of hydrophobic interactions (Fig. 4). These interactions are listed in Table II and will be discussed in more detail in the following section. The contribution of the various residues to the ancillary pocket is listed in Table III.

No electron density is present for BtUSP residues prior to Val-300 (*i.e.* for residues prior to the N terminus of helix H3). The absence of these residues most likely results from the proteolytic loss of residues prior to BtUSP Leu-285 (see "Materials and Methods") with consequent destabilization of BtUSP residues Leu-285 to Pro-299. Comparison with other USP-LBD structures indicates that BtUSP residue Leu-285 lies at the approximate midpoint of helix H1 in those structures. No ligand is bound in our BtUSP-LBD structure, and helix H12 lies in the canonical antagonist conformation.

A large electron-dense feature within the BtEcR-LBD/

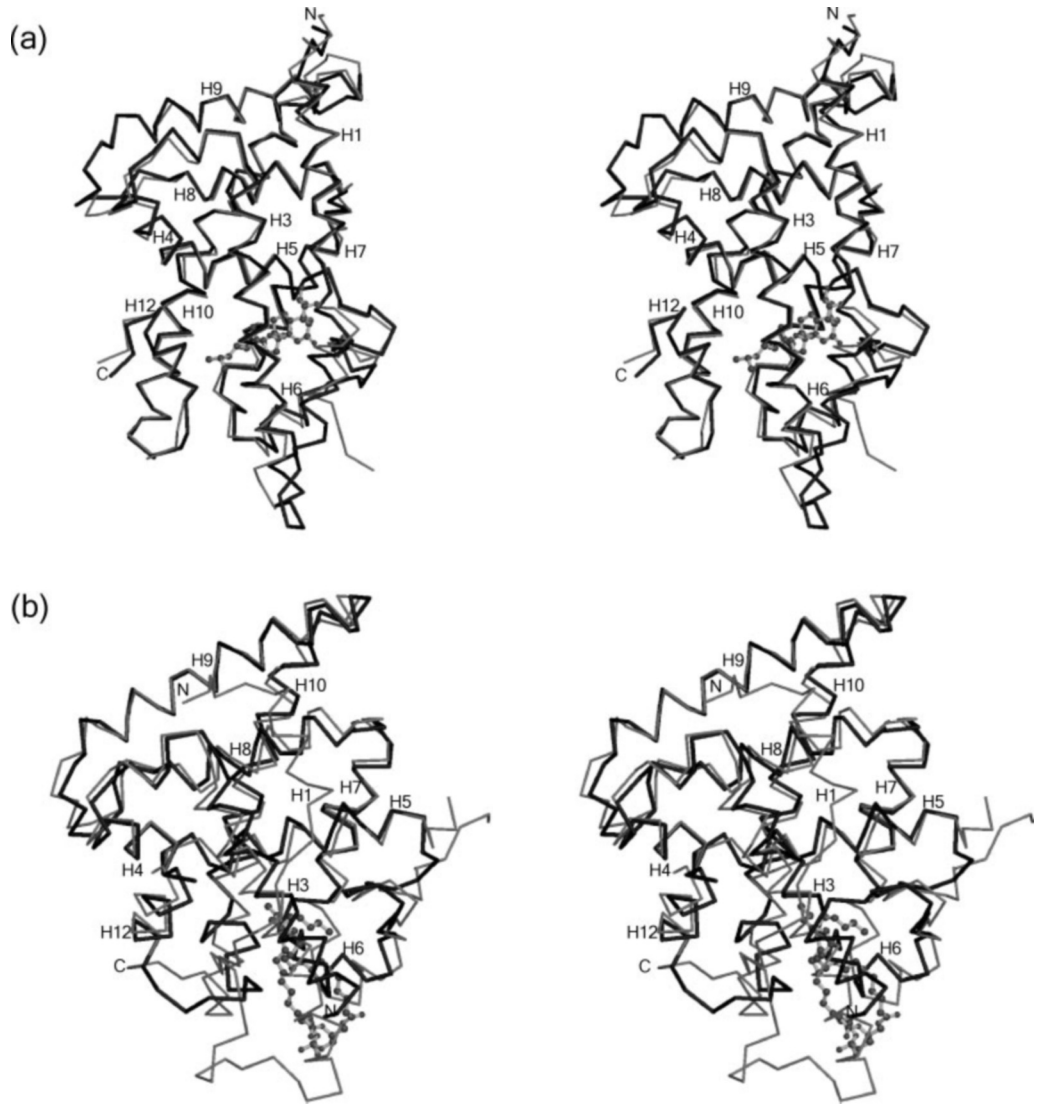

FIG. 3. **Stereoviews of overlaid C$^{\alpha}$ backbone traces of the *B. tabaci* and *H. virescens* ecdysone receptor LBDs.** *a*, BtEcR-LBD (*black lines*) and HvEcR-LBD (*gray lines*). The location of the ligand PonA is effectively identical in both LBD structures and is shown in *ball-and-stick* representation. *b*, BtUSP-LBD (*black lines*) and HvUSP-LBD (*gray lines*). Also shown is the location of the bound phospholipid in the HvUSP-LBD structure (*ball-and-stick* representation). The absence of helix H1 and the helix H1 to helix H3 connection is apparent in the BtUSP-LBD as well as the movement of the helix H6 to helix H7 loop and the helix H10 to helix H12 loop into the volume occupied by lipid in the HvUSP-LBD structure. The canonical α-helices H1–H12 are labeled in both *a* and *b* as are the observed N and C termini. The figure was produced using MOLSCRIPT (54) and RASTER-3D (56).

BtUSP-LBD heterodimer interface was modeled as a single phosphate ion, coordinated by the side chain of Arg-384 in BtEcR and the side chains of Arg-383 and Arg-456 in BtUSP. The source of this ion is potentially the crystallization mother liquor (see "Materials and Methods"), and its physiological relevance, if any, is thus unclear.

Comparison of the Structures of BtEcR-LBD and HvEcR-LBD—The overall structures of the PonA-bound LBDs of BtEcR and HvEcR are closely similar as anticipated by their ~56% sequence identity (Fig. 5). Their polypeptide backbones can be overlaid with a root mean square deviation of 1.1 Å for 228 corresponding C$^{\alpha}$ atoms out of a total of 241 (Fig. 3). Differences in backbone conformation are restricted to loop regions in particular (i) the helix H2 to helix H3 loop with the loop in BtEcR being two residues shorter than its HvEcR counterpart, (ii) the helix H8 to helix H9 loop, and (iii) the helix H9 to helix H10 loop. The stereochemical conformation of the bound PonA is effectively identical in the two structures. The volume of the entire BtEcR-LBD pocket is ~766 Å^3 of which about 650 Å^3 comprise the major pocket and 116 Å^3 comprise the ancillary pocket. Although the PonA-bound HvEcR-LBD ligand-binding pocket does not exhibit an extension equivalent to the ancillary pocket of the BtEcR-LBD, our inspection of that structure reveals the existence of a previously unobserved cavity in a location equivalent to that of the ancillary pocket in BtEcR-LBD but unconnected to the PonA-binding pocket (Figs. 6*b* and 7*a*). For ease of comparison, we nevertheless refer to the PonA-binding pocket of the HvEcR-LBD as the major pocket and the smaller disjoint cavity as the ancillary pocket. The respective volumes of these two HvEcR-LBD pockets are 639 and 103 Å^3, *i.e.* comparable in sum to the single BtEcR-LBD pocket. The relative loss of connectivity of the major and ancillary pockets in HvEcR-LBD is a consequence of differing rotameric conformations of the side chains of Glu-309 and Arg-516 compared with their BtEcR equivalents (Glu-119 and Arg-402, respectively). The ancillary pockets in both the BtEcR-LBD and HvEcR-LBD structures appear unoccupied, although we note that the limited resolution of these structures (3.1 and 2.9 Å, respectively) precludes the detection of small or weakly ordered solvent molecules.

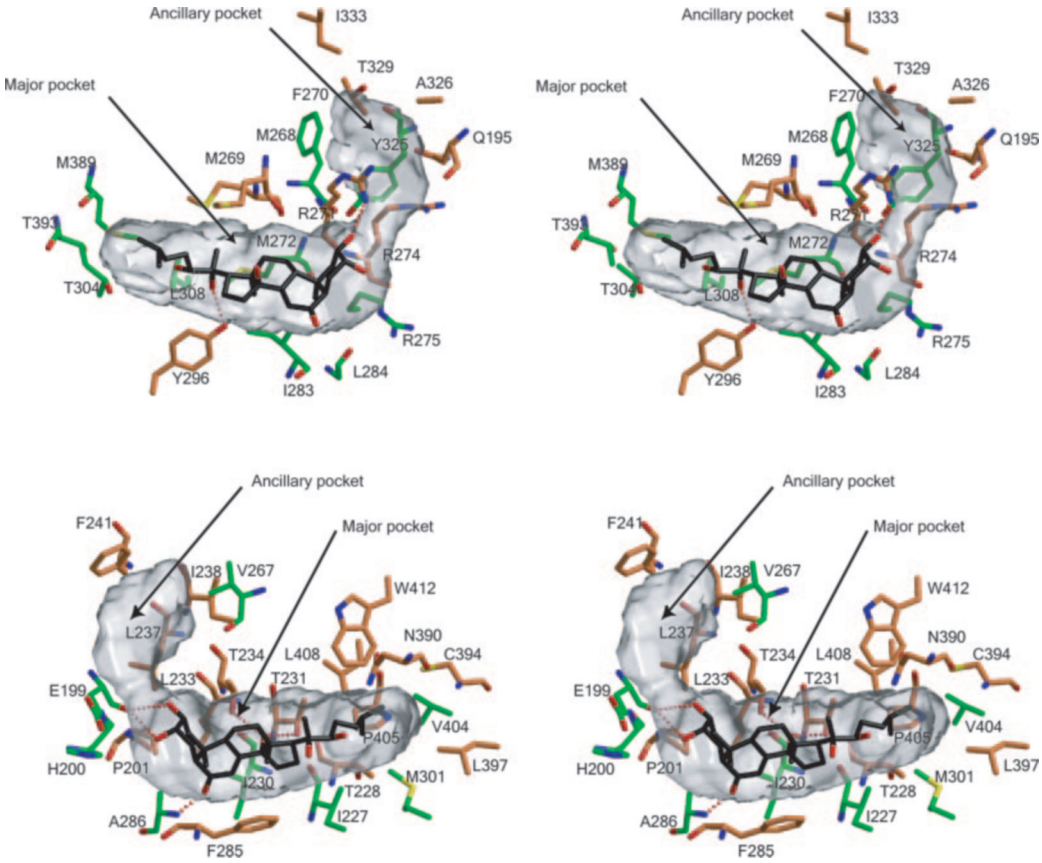

FIG. 4. **Stereoviews of the opened out ecdysteroid-binding pocket of BtEcR.** The intact pocket is regenerated by rotating each of the lower pair of images by 180° about a vertical in-page axis and placing them on top of the upper pair of images. PonA is shown with *black* bonds, *black* carbon atoms, and *red* oxygen atoms. Surrounding residues (with selected side chain or main chain groups omitted for clarity if their atoms do not contribute to the cavity wall) are shown with *orange* carbon atoms if conserved across all EcR sequences considered in the construction of Tables II and III; otherwise they are shown with *green* carbon atoms. *Red dotted lines* show hydrogen bonds between the BtEcR-LBD and PonA. The molecular surface of the ligand-binding pocket is in *transparent gray* and is concave in each stereopair, corresponding to the opening out and removal of the respective upper portion of the pocket. The figure was produced using MOLSCRIPT (54), CONSCRIPT (55), and RASTER-3D (56).

We now turn to a more detailed comparison of the PonA-binding pockets of the BtEcR-LBD and the HvEcR-LBD based on the analysis presented in Table II. Seven potential hydrogen bonds are formed between the ligand and the receptor in each case and involve identical residues in the two structures. Where these interactions involve residue side chain atoms, the rotameric conformations of the side chains are effectively identical in the two structures. Furthermore almost all of the residues involved in these interactions are completely conserved across insect orders. Eighteen BtEcR residues have side chains that are in non-polar interaction with PonA. Fifteen of these residues are conserved in HvEcR and display equivalent rotamer conformations and make somewhat similar area contributions to the pocket surface in both structures. Three of the BtEcR residues that are in non-polar interaction with PonA are not conserved in HvEcR, and the effect of these substitutions on the pocket wall is as follows. The replacement of BtEcR Ile-230 by HvEcR Met-342 resulted in an ~1-Å deeper intrusion of the pocket wall into the protein atomic volume adjacent to PonA atom C-4. The replacement of BtEcR Met-272 by HvEcR Val-384 and of BtEcR Ile-283 by HvEcR Val-395 had no significant effect on the pocket geometry at these locations. However, in the instance of the BtEcR Met-272/HvEcR Val-384 substitution, conservation of pocket geometry was mediated in part by the rearrangement of the side chain of the structurally adjacent, conserved, and non-ligand-interacting residue BtEcR Leu-308 (see below). Further inspection of Table II shows that these 15 conserved non-polar residues identified in the BtEcR-LBD structure are also highly conserved across available EcR sequences of hemipteran, lepidopteran, dipteran, and coleopteran orders. In summary, therefore, we conclude that the parts of the ligand-binding pocket surface in contact with the PonA ligand appear remarkably well conserved in the *B. tabaci* and *H. virescens* structures not only in shape but also in overall hydrophobic and polar character. Based on the interorder EcR sequence variation presented in Table II, the conservation of shape and character of the PonA-interacting surface likely persists across the Arthropoda.

However, the same is not true of those parts of the major binding pocket formed by residues that do not contribute to the interaction with the PonA ligand. Nine BtEcR residues that contribute atoms to the formation of the surface of the major pocket do not interact directly with PonA. Three of these residues (*viz.* BtEcR His-200, Arg-274, and Leu-284) contribute to the pocket surface in the vicinity of the A-ring of the ligand. Of these, BtEcR Arg-274 is conserved as HvEcR Arg-386, and although the modeled rotameric conformation of these residues differ, their side chains lie in similar locations with respect to the ligand-binding pocket. We note that BtEcR Arg-274 (HvEcR Arg-386) is involved in charged interaction with BtEcR Glu-199 (HvEcR Glu-309), and it is the differing conformation of the respective glutamate side chains that leads to the severing of the major and ancillary pockets in the HvEcR-LBD. BtEcR His-200 makes only a small contribution to the pocket surface, whereas its counterpart HvEcR Gln-310 makes no contribution at all. BtEcR Leu-284 is conserved as HvEcR Leu-396, and because only the main chain atoms of each of these residues contribute to the pocket surface, no appreciable

TABLE II

Residues forming the major ligand binding pockets of BtEcR- and HvEcR-LBDs and their conservation across insect orders

The alignment data for the hemipteran (Hemip.), lepidopteran (Lepidop.), dipteran (Dip.), and coleopteran (Coleop.) EcR residues shown were extracted from a sequence alignment of the following EcR sequences: the hemipteran sequence of *B. tabaci* and a further in-house hemipteran sequence (Noyce, L., Eaton, R. E., Graham, L. D., Hannan, G. N., and Hill, R. J., in preparation; Pawlak-Skrzecz, A., Hannan, G. N., Graham, L. D., Hales, D. F., and Hill, R. J., in preparation); the lepidopteran sequences of *Choristoneura fumiferana* (AAC61596), *Bombyx mori* (AAA87340), *Manduca sexta* (ECR_MANSE), *H. virescens* (ECR_HELVI), *Junonia coenia* (Q9U0R9), *Bicyclus anynana* (Q9U3U4), and *Chilo suppressalis* (Q8MYA7) and a further in-house lepidopteran (*H. armigera*) sequence (Earnshaw, R., Noyce, L., Hannan, G. N., Simpson, A. M., and Hill, R. J. in preparation); the dipteran sequences of *Chironomus tentans* (ECR_CHITE), *Aedes albopictus* (Q9U3Y4), *Ceratitis capitata* (O76827), *L. cuprina* (ECR_LUCCU), *Anopheles gambiae* (EAA00117), *Calliphora vicina* (Q9GPH1), and *D. melanogaster* (ECR_DROME); and the coleopteran sequence of *Tenebrio molitor* (O02035), citing the appropriate GenBank™ or Swiss-Prot data base accession code or locus in parentheses.

BtEcR residue	Surface area MC/SC[a]	HvEcR residue	Surface area MC/SC	Rotamer conservation[b]	Interaction with PonA	Hemip.	Lepidop.	Dip.	Coleop.
	Å²		Å²						
Glu-199	15/22	Glu-309	20/20	n	O ↔ 2-OH, 3-OH	Glu	Glu, Asp	Glu	Glu
Thr-231	0/29	Thr-343	4/33	y	O^{γ} ↔ 14-OH	Thr	Thr	Thr	Thr
Thr-234	2/35	Thr-346	3/37	y	O^{γ} ↔ 14-OH	Thr	Thr	Thr	Thr
Arg-271	16/62	Arg-383	8/64	(y)	$N^{\eta 1}$ ↔ 2-OH	Arg	Arg	Arg	Arg
Ala-286	7/11	Ala-398	6/10		N ↔ 6=O	Ala	Ala	Ala	Val
Tyr-296	0/29	Tyr-408	0/27	y	O^{η} ↔ 20-OH	Tyr	Tyr	Tyr	Tyr
Pro-201	0/14	Pro-311	0/14	y	vdW[c]	Pro	Pro	Pro	Pro
Ile-227	8/18	Ile-339	4/12	y	vdW	Ile, Leu	Ile	Ile	Thr
Thr-228	6/15	Thr-340	5/13	y	vdW	Thr	Thr	Thr	Thr
Ile-230	0/24	Met-342	7/23	N	vdW	Ile, Met	Met	Ile, Val	Ile
Leu-233	0/5	Leu-345	0/6	(y)	vdW	Leu	Leu	Leu	Leu
Leu-237	0/9	Leu-349	0/6	(y)	vdW	Leu	Leu	Leu	Leu
Met-268	4/30	Met-380	8/26	y	vdW	Met	Met	Met	Met
Met-269	4/21	Met-381	0/18	y	vdW	Met	Met	Met	Met
Arg-271	16/62	Arg-383	8/64	(y)	vdW	Arg	Arg	Arg	Arg
Met-272	10/36	Val-384	7/20	N	vdW	Met, Val	Val	Met	Met
Arg-275	0/27	Arg-387	0/26	(y)	vdW	Arg, Lys	Arg	Arg	Arg
Ile-283	0/21	Val-395	0/12	N	vdW	Ile	Val	Ile	Ile
Phe-285	8/28	Phe-397	6/28	y	vdW	Phe	Phe	Phe	Phe
Ala-286	7/11	Ala-398	6/10		vdW	Ala	Ala	Ala	Val
Met-301	0/25	Met-413	0/27	(y)	vdW	Met, Leu	Met, Phe	Met, Val	Met
Cys-394	0/12	Cys-508	0/24	y	vdW	Cys	Cys	Cys	Cys
Leu-397	0/14	Leu-511	0/11	y	vdW	Leu	Leu	Leu	Leu
Trp-412	0/14	Trp-526	0/12	y	vdW	Trp	Trp	Trp	Trp
His-200	0/9	Gln-310	0/0	N	None	His, Ala	Gln	Gln	His
Arg-274	0/25	Arg-386	0/10	(y)	None	Arg	Arg	Arg	Arg
Leu-284	5/0	Leu-396	8/0	n	None	Leu, Val	Leu, Met	Phe	Leu
Thr-304	0/13	Val-416	6/31	N	None	Thr, Ala, Val	Val	Asn, Thr	Thr
Leu-308	2/38	Leu-420	0/26	n	None	Leu, Gln	Leu	Leu	Leu
Met-389	0/12	Gln-503	0/9	N	None	Met, Glu, Gln	Gln	Gln, Lys	Gln
Thr-393	0/22	Met-507	0/16	N	None	Thr, Leu, Met	Met	Met	Met
Val-404	0/10	Leu-518	0/24	n	None	Val, Leu	Leu	Leu	Leu
Leu-408	0/10	Leu-522	3/19	(y)	None	Leu	Leu	Leu	Leu

[a] MC/SC, surface area contributed to the pocket wall by residue main chain atoms and residue side chain atoms, respectively.

[b] The following scheme is used to indicate side chain rotamer conservation: y, rotamer conserved; n, rotamer not conserved; (y), rotamer not conserved but side chains occupy similar volumes; N, residue not conserved.

[c] vdW, van der Waals.

TABLE III

Residues forming the ancillary pockets of BtEcR- and HvEcR-LBDs and their conservation across insect orders

The interorder residue variation was derived from the same sequence alignment used in the construction of Table II. Hemip., hemipteran; Lepidop., lepidopteran, Dip., dipteran; Coleop., coleopteran.

BtEcR residue	Surface area MC/SC[a]	HvEcR residue	Surface area MC/SC	Hemip.	Lepidop.	Dipt.	Coleop.
	Å²		Å²				
Gln-195	14/19	Gln-305	13/26	Gln	Gln	Gln	Gln
Ile-238	8/7	Ile-350	3/17	Ile	Ile	Ile	Ile
Phe-241	0/33	Phe-353	0/32	Phe	Phe	Phe	Phe
Val-267	0/19	Val-379	0/9	Val, Ala	Val	Val	Val
Phe-270	2/8	Leu-382	2/7	Phe, Leu	Leu	Leu	Phe
Arg-274	0/25	Arg-386	0/10	Arg	Arg	Arg	Arg
Tyr-325	0/3	Tyr-437	0/7	Tyr	Tyr, Phe	Tyr	Tyr
Ala-326	0/4	Ala-438	0/7	Ala	Ala	Ala	Ala
Thr-329	0/22	Thr-441	0/24	Thr	Thr	Thr	Thr
Ile-333	6/5	Ile-445	0/6	Ile	Ile	Ile	Ile

[a] MC/SC, surface area contributed to the pocket wall by residue main chain atoms and residue side chain atoms, respectively.

change in pocket geometry was observed at this location. The six remaining residues contributing to the pocket surface but not interacting with the ligand (*viz.* BtEcR Thr-304, Leu-308, Met-389, Thr-393, Val-404, and Leu-408) lie in the vicinity of the alkyl tail of PonA. Of these six residues, only Leu-308 and Leu-408 are conserved in HvEcR (as Leu-420 and Leu-522, respectively); however, the rotameric conformation of the side chain of BtEcR Leu-308 differs significantly from that of its HvEcR counterpart. The combined effect of these five substitutions and the relative rotameric change at the BtEcR Leu-

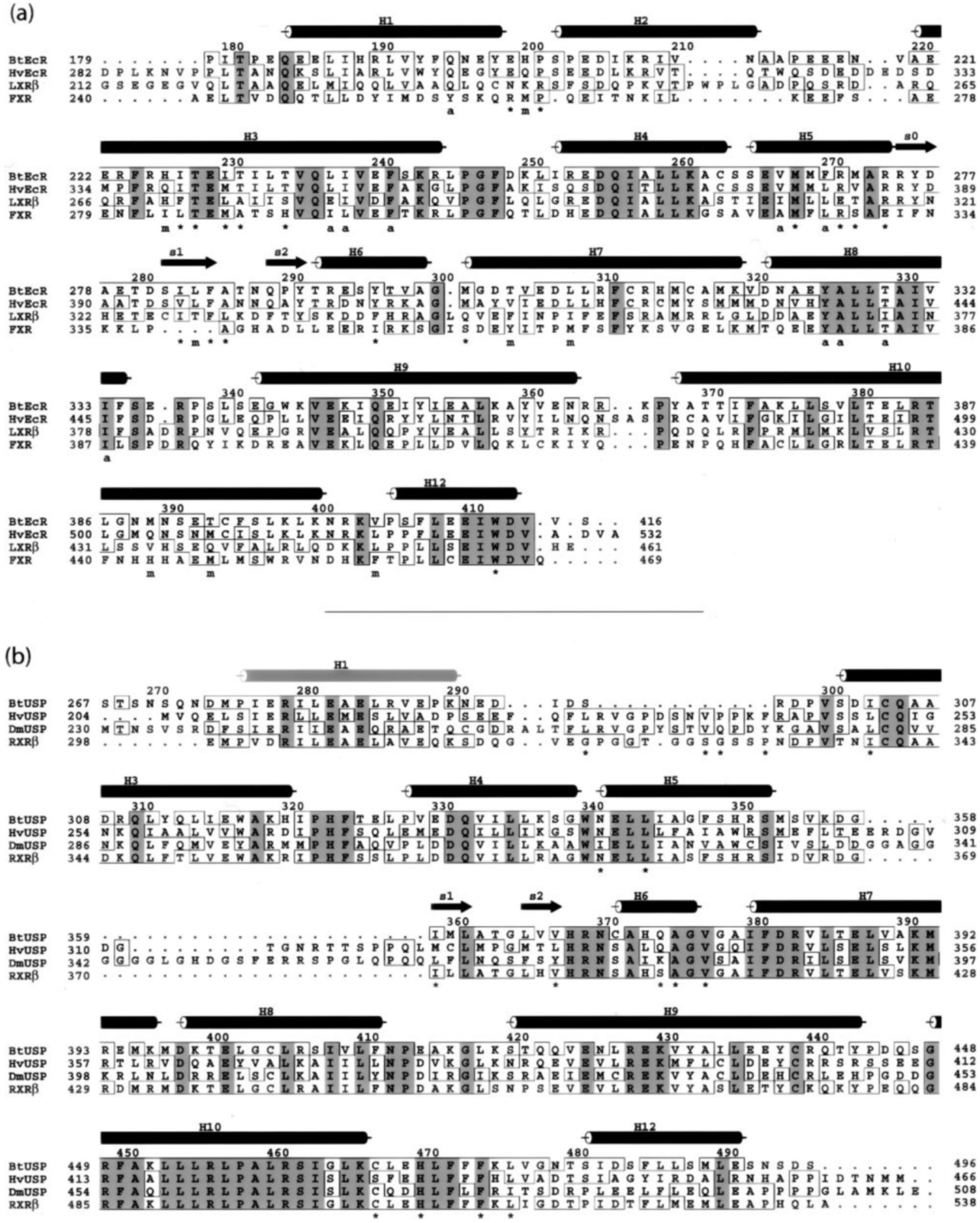

FIG. 5. **Sequence alignment of the LBDs of BtEcR, HvEcR, LXR*β*, and FXR (*a*) and BtUSP, HvUSP, DmUSP, and RXR*β* (*b*).** Included in the alignment are the location of the secondary structural elements observed in the BtEcR-LBD heterodimer structure presented here (helices are shown as *cylinders*; strands are shown as *arrows*). Helix H1 in *b* is unobserved in our BtUSP-LBD structure (see text), and its location is based upon the HvUSP-LBD structure. Residues *highlighted* against a *gray background* are conserved in all four sequences in each alignment block, whereas those *highlighted* by *outlining* are conserved in two or three of the sequences within each alignment block. Indicated *underneath* the EcR-LBD alignment are the residues contributing to the surface of the ecdysteroid-binding pocket within the BtEcR-LBD (*, major pocket residue in contact with PonA; *m*, major pocket residue not in contact with PonA; *a*, ancillary pocket residue). Indicated (*) *beneath* the USP-LBD alignment are residues involved in lipid contact in HvUSP-LBD. The sequences shown are those of the respective Protein Data Bank structures: *a*, entries 1Z5X (this work), 1R1K, 1P8D, and 1OSV; and *b*, entries 1Z5X (this work), 1R1K, 1HG4, and 1UHL. Residues shown in *lowercase* are missing in the respective Protein Data Bank entry. The alignment was generated using ClustalW (57), and the figure was produced using ALSCRIPT (58).

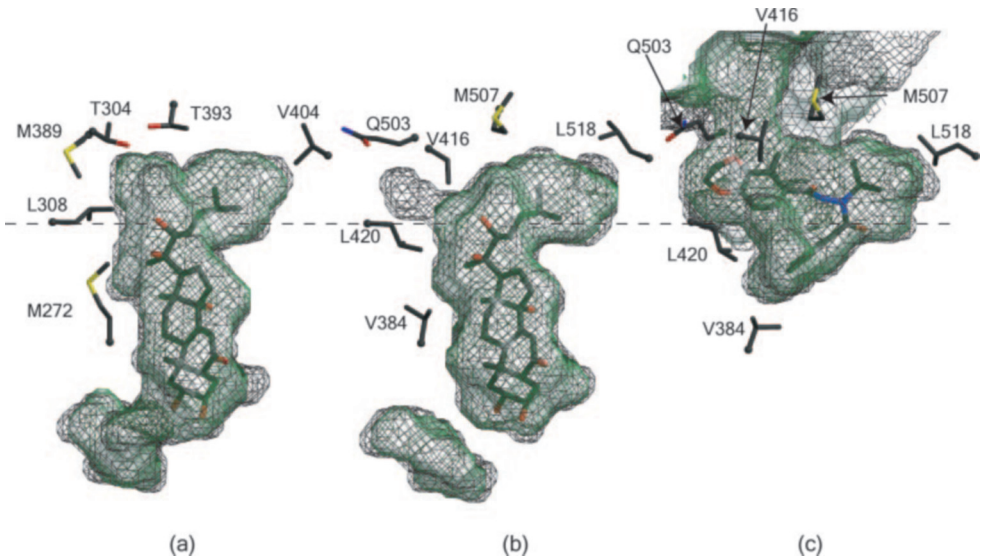

FIG. 6. **The ligand-binding pockets of the BtEcR-LBD showing PonA bound (*a*), HvEcR-LBD showing PonA bound (*b*), and HvEcR-LBD showing BYI06830 bound (*c*).** All pockets are shown in equivalent orientations for ease of comparison with the *dotted line* tracing through a common coordinate. The side chains of selected residues discussed in the text are shown in *stick* representation with C^{α} atoms shown as small *spheres*. Pockets were generated using VOIDOO (30) both with the default 1.4-Å probe radius (*transparent green*) and a 1.2-Å probe radius (*black mesh*) in an endeavor to locate more loosely packed regions of the pocket wall. The looser packing of the walls of the HvEcR-LBD ligand-binding pocket in the vicinity of residues Leu-420, Val-416, and Gln-503 is evidenced by both by the orientation of the side chains of these residues and by the intrusion into the protein atomic volume of the ecdysteroid-binding pocket wall calculated with a 1.2-Å probe radius. The opening up of this region upon BYI06830 binding is evident in *c* with the pocket volume now opening outward to solvent. No such region of looser packing is evident in the walls of the ligand-binding pocket of BtEcR-LBD. The figure was produced using MOLSCRIPT (54), CONSCRIPT (55), and RASTER-3D (56).

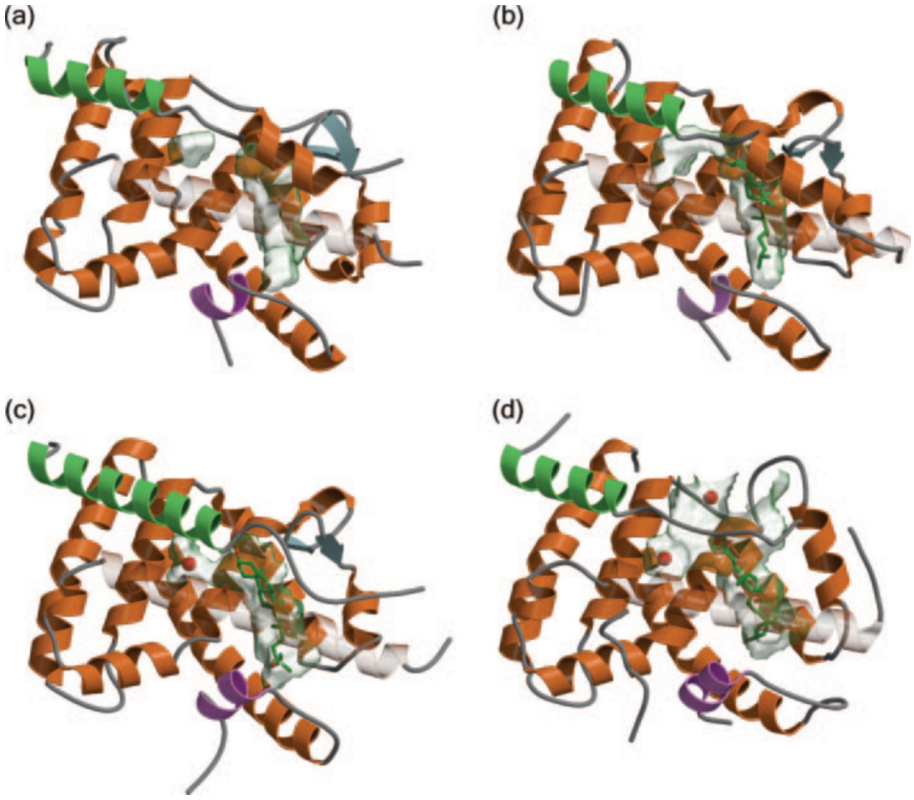

FIG. 7. **Ligand-binding pockets of HvEcR-LBD complexed with PonA (16) (Protein Data Bank entry 1R1K) (*a*), BtEcR-LBD complexed with PonA (*b*), LXRβ complexed with 24(*S*),25-epoxycholesterol (47) (Protein Data Bank entry 1P8D) (*c*), and FXR complexed with 6-ethyl-chenodeoxycholic acid (48) (Protein Data Bank entry 1OSV) (*d*).** All LBDs are shown in equivalent orientations for ease of comparison. Pockets were calculated using VOIDOO (30) with the default 1.4-Å probe radius and are shown in *transparent green*. Ligands are shown in *cyan*, and bound water molecules are shown in *red*. Helices are shown in *orange* except for helix H1, which is shown in *green*, and helix H12, which is shown in *mauve*. Helix H3 is rendered *transparent* to allow viewing of the pockets. In *c*, the ancillary pocket, when computed with a probe radius of 1.2 Å (not shown), opens to the surface as in *d*. The figure was generated using MOLSCRIPT (54), CONSCRIPT (55), and RASTER-3D (56).

308 position produces a significant difference in the pocket shape and structure in this vicinity (Fig. 6) that will be described in more detail in the next section. We suggest that this difference in architecture may underlie the differential affinity of the hemipteran and lepidopteran EcR-LBDs for the bisacylhydrazine compounds.

In the BtEcR-LBD and HvEcR-LBD PonA-bound structures, the interaction of helix H12 with PonA is limited to a van der Waals interaction between the ring of the conserved tryptophan at position BtEcR Trp-412 (HvEcR Trp-526) and the terminus of the PonA alkyl tail. The interactions between helix H12 and the remainder of BtEcR-LBD include (i) a conserved salt bridge between the side chains of BtEcR Asp-413 (HvEcR Asp-527) at the C terminus of helix H12 and BtEcR Lys-261 (HvEcR Lys-373) within helix H4 and (ii) a conserved polar interaction between BtEcR Trp-412 $N^{\epsilon 1}$

(HvEcR Trp-526) and the hydroxyl of BtEcR Ser-264 (HvEcR Ser-376) within helix H5. The conserved salt bridge between helices H12 and H4 appears equivalent to that observed between the same elements in agonist-bound vertebrate NRs (36), although in the latter cases the salt bridge uses a glutamate located one turn closer to the N terminus of helix H12 (equivalent to BtEcR Glu-410).

Bisacylhydrazine Specificity—The above analysis reveals that significant differences in ligand-binding pocket geometry arise in the vicinity of the residues that are not in contact with PonA in particular in the vicinity of BtEcR Thr-304, Leu-308, Met-389, Thr-393, Val-404, and Leu-408. In BtEcR-LBD, the rotameric conformations of Met-389 (within helix H10) and Leu-308 (within helix H7) place the side chains of these residues in contact with each other (Fig. 6*a*). In the HvEcR-LBD, the rotameric conformations of the equivalent residues (Gln-503 and Leu-420, respectively) are distinctly different (Fig. 6*b*). Indeed the side chain of HvEcR Gln-503 is oriented away from the bound ligand with its terminal amide group exposed on the outer surface of the protein, whereas the side chain of HvEcR Leu-420 is directed toward HvEcR residue Val-384. These arrangements are indicative of a weaker interaction at this location between helices H7 and H10 in the HvEcR-LBD compared with that in BtEcR-LBD. Pocket surface calculations with a probe radius of 1.4 Å revealed a small indentation of the pocket wall into the HvEcR-LBD protein volume between residues Val-416, Leu-420, and Gln-503 (Fig. 6*b*) that is absent in BtEcR-LBD (Fig. 6*a*). Calculation of the pocket surface with a 1.2-Å probe, however, revealed a larger extraversion of the pocket in this region. Intriguingly it is precisely here that the 1,4-dioxan ring of BYI06830 inserts itself into the protein atomic volume (Fig. 6*c*). Given the high level of structural conservation in those regions of the ligand-binding pocket that interact with the ecdysteroid PonA, it appears that it is the structural variability in the vicinity of this indentation (which does not interact directly with the ecdysteroid) that may underpin the differential binding affinity of the bisacylhydrazine compounds across taxonomic orders. We note that the structural variability is not derived from any single amino acid substitution but instead probably reflects the combined effect of coordinated residue substitutions on an order-by-order basis.

A number of other changes to the pocket architecture of the HvEcR-LBD accompany the binding of BYI06830 (16). The first of these is a disruption of the hydrogen bond interactions between the second and third strands of the β-sheet, allowing the inward motion of the aromatic side chains of residues Phe-397 and Tyr-403, which then fill that part of the binding cavity otherwise occupied by the A-, B-, and C-rings of PonA in the ecdysteroid-bound structure of HvEcR-LBD. Both of these aromatic residues are conserved in BtEcR (as Phe-285 and Tyr-291, respectively), and these positions are also conserved as aromatics in known EcR sequences (Table II). However, we note that the residue N-terminal to HvEcR Tyr-403, *viz.* Ala-402, is a proline in BtEcR (Pro-290) and in other hemipteran EcRs. This change may restrict backbone flexibility in this region and prevent the rearrangements necessary to accommodate a compound such as BYI06830 in the manner seen in HvEcR-LBD. Lepidopteran and dipteran EcR sequences appear to have serine and alanine residues at this position, and these orders are susceptible to bisacylhydrazine insecticides (10, 37). However, we note that Coleoptera are susceptible to bisacylhydrazines (10) but that the only available coleopteran sequence retains a proline at this position. Hence the presence of a proline at this position cannot by itself account for the poor ability of the corresponding LBDs to bind bisacylhydrazine compounds. The remaining structural change in HvEcR-LBD upon binding of BYI06830 is the destabilization of helix H2, directing the side chain of Gln-310 into that part of the pocket occupied by the ligand A-ring in PonA-bound HvEcR-LBD. This residue is conserved as a glutamine in dipteran and lepidopteran EcR sequences but is substituted either by smaller residues (alanine or serine) or by residues having fewer conformational degrees of freedom (histidine) in EcR sequences from other insect orders. This suggests that in a hemipteran EcR-LBD these residues may be unable to fill in the unoccupied volume that arises in this region upon bisacylhydrazine binding. Finally we note that three HvEcR residues (*viz.* Thr-343, Tyr-408, and Asn-504) form polar interactions with BYI06830 and that these residues are highly conserved in EcR sequences across all orders. The BtEcR equivalents of these three residues are Thr-231, Tyr-296, and Asn-390, respectively, and inspection reveals that these residues enjoy conformations similar to their HvEcR counterparts in the respective PonA-bound structures. It is thus unlikely that these residues are responsible for the very different bisacylhydrazine affinities exhibited by these two receptors.

Binding Activity of Other Ecdysteroids—Extensive studies of the relative binding activities of various ecdysteroids to the ecdysone receptor have been reported in the literature. Structural interpretation must necessarily be cautious given the flexibility of the ecdysteroid-binding pocket and the use of different assay techniques (predominantly bioassays, the results of which need not directly reflect the affinity of the ecdysone receptor LBD heterodimer for the ligand). Nevertheless the existing LBD structures do provide insight into the degree of substitution tolerated within the ecdysteroid ring system. For example the interaction between the 20-hydroxyl group of PonA and the hydroxyl group of the conserved residue HvEcR Tyr-408 (BtEcR Tyr-296) almost certainly underpins the well established higher activity of ecdysteroids possessing a 20-hydroxyl group, in particular the increased activity of the native hormone 20-hydroxyecdysone over ecdysone for dipteran and lepidopteran receptors (38). A similar hydrogen bond interaction between PonA and a tyrosine residue was observed in the corresponding HvEcR structure (16). Polypodine B (a phytoecdysteroid) contains an additional β-hydroxyl substituent at C-5 within the ecdysteroid ring and exhibits higher activity relative to 20-hydroxyecdysone in the case of the Dm receptor (39). This increased activity may result from the C-5 β-hydroxyl group forming a hydrogen bond with (BtEcR) Arg-275 N^{ϵ}, a residue conserved in both HvEcR and DmEcR. Ecdysteroids with an α-hydroxyl substituent at C-11 show reduced activity (39), and inspection of the ligand-binding pocket of our structure and that of the PonA-bound *H. virescens* ecdysone receptor LBD heterodimer suggests that such a substituent cannot readily be accommodated without some alteration to the pocket geometry. The reduced activity of malacosterone (20-hydroxyecdysone with a β-hydroxyl at the C-16 position) in *D. melanogaster* (39) is potentially explained by a clash of the additional hydroxyl with the side chain hydroxyl of Tyr-296 in the BtEcR-LBD or of Tyr-408 in the HvEcR-LBD. In the same study, the relative activities of ecdysteroids with methyl substituents near the terminus of the alkyl tail appeared to have no effect or to slightly increase their binding affinity for EcR. However, modeling their mode of binding would be daunting in that one would have to allow for (i) the alkyl tail potentially adopting a different conformation, (ii) the residues lining the ligand pocket adopting altered rotameric conformation, and/or (iii) more extreme change in the conformation of the pocket to accommodate the substituent, as seen in the complex of the *H. virescens* LBD heterodimer with BYI06830.

Comparison of the BtUSP-LBD and HvUSP-LBD Structures—The polypeptide backbones of BtUSP-LBD and HvUSP-LBD (Fig. 3*b*) are closely similar in conformation (1.3-Å root

mean square deviation for 169 corresponding C^{α} atoms out of 193). All three previously determined USP-LBD crystal structures display phospholipid bound in a cleft partly overlaying the canonical location of the hormone-binding pocket within the NR fold (16–18); no lipid is, however, observed bound to BtUSP-LBD. This absence of lipid appears to correlate with a number of conformational differences in the vicinity of the putative ligand-binding pocket in BtUSP-LBD compared with its HvUSP-LBD and DmUSP-LBD counterparts, and these differences will now be described. In the HvUSP-LBD structure, the lipid is bound in a cleft, the walls of which are formed by residues located within (i) the loop connecting helix H6 to helix H7, (ii) the N-terminal portion of helix H3 and part of its connection to H1, and (iii) the C terminus of helix H10. The hydrophobic tails of the lipid are directed into this cleft, whereas the polar head group protrudes out of the LBD. The site of protrusion is structurally distinct from that "capped" by helix H12 when in the agonist position. In the BtUSP-LBD structure, volume equivalent to that forming the lipid-binding cleft in HvUSP-LBD is occluded by a "folding in" of the loop connecting helix H6 to helix H7 (Fig. 3*b*). There is also a folding in of the loop connecting helix H10 to helix H12 into volume that might otherwise be occupied by the connection between helix H1 and helix H3 in an intact LBD. Part of the "folded in" helix H10 to helix H12 loop also overlays volume equivalent to that forming the lipid-binding cleft in HvUSP-LBD. Similar observations arise upon comparison of our structure with that of *D. melanogaster* USP-LBD monomer (17).

The reason for the absence of bound lipid in BtUSP-LBD is not clear. Inspection of the sequence alignment of the LBDs of BtUSP and HvUSP (Fig. 5*b*) revealed that of the 16 residues that are in contact with lipid (3.8-Å cutoff) in HvUSP-LBD nine (Asn-287, Leu-290, Gln-338, Ala-339, Val-341, Ser-431, His-434, Phe-438, and Leu-440) are conserved and three (Leu-249, Met-323, and Leu-331) are conservatively replaced in the BtUSP sequence (Ile-303, Ile-359, and Val-367, respectively). Four residues (Leu-230, Val-238, Pro-239, and Phe-242) are missing in the shortened BtUSP sequence region between helix H1 and helix H3. Three explanations may thus be advanced for the absence of bound lipid in BtUSP-LBD. One possibility is that although lipid may bind to an intact BtUSP-LBD, the absence of all BtUSP residues prior to Leu-285 (see above) makes collapse of the helix H6 to helix H7 loop into the lipid-binding region more energetically favorable than lipid binding itself. The folding in of the loop connecting helix H10 to helix H12 also appears feasible in the absence of residues prior to Leu-285 and may be mediated in part by the observed involvement of that loop in a crystal contact. A further possibility is that the lipids seen in other USP-LBDs arise as a consequence of bacterial expression and are not observed here because the recombinant receptor was expressed in insect cells (see "Materials and Methods"). A third explanation is that intact BtUSP-LBD is structurally distinct from HvUSP-LBD and DmUSP-LBD in a way that precludes lipid binding. Indeed we note that part of the lipid-binding cavity in HvUSP-LBD is formed by three residues (HvUSP Val-238, Pro-239, and Phe-242) in the 13-residue insertion that is present in the HvUSP sequence but not in that of the BtUSP (Fig. 5*b*). The path of this loop must, therefore, be different in the two USP-LBDs and possibly allows the observed rearrangement of the helix H10 to helix H12 connection in BtUSP-LBD compared with HvUSP-LBD. We note further that if the structure of the helix H10 to helix H12 loop observed here corresponds to a native-like antagonist conformation of helix H12, then the helix H10 to helix H12 loop will have to undergo significant rearrangement if helix H12 were to move to a classical agonist position. The absence of residues prior to BtUSP Leu-285 in our structure, however, precludes us from commenting further on whether or not helix H12 is locked (17, 18) in the antagonist conformation observed.

It has been pointed out (40) that the USP-LBDs of the Panorpida (which includes the dipteran and lepidopteran orders) are more distant from the chordate RXR-LBDs than are the USP-LBDs of other insect orders. Indeed we note that BtUSP bears a closer sequence relationship to human RXR than to HvUSP (Fig. 5*b*) in the regions responsible for lipid binding. The RXR-LBD can bind fatty acids in this location regardless of the conformation of the loop connecting helix H1 to helix H3 (24, 41) so this distinction between USP-LBD sequences of different orders is unlikely to explain the absence of bound lipid in our structure.

Comparison of the Ecdysone Receptor LBD Heterodimeric Interfaces—The overall mode of assembly of the *B. tabaci* and *H. virescens* ecdysone receptor LBD heterodimers is very similar, brought about primarily by a pseudo 2-fold interaction between the helices H9 and H10 in the EcR-LBD with the corresponding helices in the USP-LBD. Some caution must, however, be exercised in comparing the detail of the interfaces of these two structures, given that the inclusion of a phosphate ion within the *B. tabaci* ecdysone receptor LBD heterodimer interface is probably a crystallization artifact that likely distorts the conformation and/or packing of the surrounding side chains compared with their structure in solution. Table IV presents the charged and polar interactions observed within the respective ecdysone receptor LBD heterodimer interfaces. Two intermolecular salt bridges and one hydrogen bond are conserved in both interfaces, but these are supplemented by a number of non-conserved salt bridges and polar interactions in each case. The *H. virescens* heterodimer interface buries about 30% more surface area than that of its *B. tabaci* counterpart (2230 *versus* 1660 $Å^2$, respectively). The larger buried surface area in the *H. virescens* heterodimer is associated with three regions in the interface. The first is in the vicinity of the loop connecting EcR helix H9 to helix H10 (Fig. 3*a*). In HvEcR-LBD, this segment is folded further into the interface than the corresponding segment in BtEcR-LBD, resulting in the burial of additional molecular surface. However, because most of this additional buried surface area is associated with contacts between this loop and the poorly ordered residue HvUSP Arg-404, it may not be significant. The side chain of the corresponding residue in BtUSP, Arg-440, adopts a rotameric conformation different than its HvUSP counterpart and is involved in an intramolecular salt bridge with Glu-436. This residue is conservatively replaced in HvUSP by Asp-400, but the reduction in side chain length does not appear to preclude the formation of an analogous intramolecular salt bridge. The second region of reduced buried surface area in the *B. tabaci* heterodimer interface relative to its *H. virescens* counterpart is in the vicinity of the loop connecting helix H10 to helix H12. In BtUSP-LBD parts of this loop are relatively disengaged from the interface. The change in conformation within this loop region has already been discussed in connection with the absence of bound lipid in BtUSP-LBD, and its significance is unclear. The third region of difference results from a reduced contact between BtUSP-LBD helix H7 and the loop connecting helices H8 and H9 in BtEcR-LBD relative to their *H. virescens* counterparts and is likely related to the incorporation of the phosphate ion in that region of the interface. Analysis of the hydrophobicity of the constituent interface surfaces of both heterodimers reveals that they are each about 55–60% hydrophobic in character, which is toward the lower end of the range associated with protein-protein inter-

TABLE IV
Interactions within the ecdysone receptor LBD heterodimeric interfaces

	BtEcR	BtUSP	*d*	HvEcR	HvUSP	*d*
			Å			Å
Conserved salt bridges	Glu-347 $O^{\epsilon1}$	Lys-391 N^{ζ}	3.0	Glu-459 $O^{\epsilon2}$	Lys-355 N^{ζ}	3.0
	Glu-382 $O^{\epsilon1}$	Arg-461 $N^{\eta2}$	4.1[a]	Glu-496 $O^{\epsilon2}$	Arg-425 $N^{\eta1}$	3.2[a]
		Arg-461 $N^{\eta1}$	3.2		Arg-425 $N^{\eta2}$	3.1
Conserved hydrogen bonds	Arg-384 $N^{\eta1}$	Ser-462 O^{γ}	3.2	Arg-498 N^{ϵ}	Ser-426 O^{γ}	3.0
Non-conserved salt bridges	Glu-336 $O^{\epsilon1}$	Lys-391 N^{ζ}	3.3			
	Glu-351 $O^{\epsilon1}$	Lys-452 N^{ζ}	3.2[b]			
	Lys-375 N^{ζ}	Glu-429 $O^{\epsilon2}$	3.2[b]			
				Arg-470 $N^{\eta2}$	Glu-411 $O^{\epsilon2}$	2.9
				Asp-448 $O^{\delta1}$	Glu-351 $O^{\epsilon2}$	2.8
				Glu-496 $O^{\epsilon1}$	Asp-378 $O^{\delta2}$	3.0
Non-conserved hydrogen bonds	Glu-355 $O^{\epsilon1}$	Ser-447 O^{γ}	3.3[b]			
	Lys-358 N^{ζ}	Ser-447 O	3.2[b]			
				His-422 $N^{\epsilon2}$	Asp-378 O	2.6
				Ser-429 O^{γ}	Arg-385 $N^{\eta1}$	2.9
				Thr-499 $O^{\gamma1}$	Arg-425 $N^{\eta1}$	2.7
				Arg-463 N^{ϵ}	Glu-411 $O^{\epsilon2}$	2.9
	BtEcR	PO_4	*d*	BtUSP	PO_4	*d*
			Å			Å
Interactions with buried phosphate ion[c]	Arg-384 $N^{\eta1}$	O-3	3.0	Arg-383 $N^{\eta1}$	O-3	2.9
	Arg-384 $N^{\eta2}$	O-2	3.0	Arg-383 $N^{\eta2}$	O-3	2.8
	Arg-384 $N^{\eta1}$	O-2	3.3	Glu-387 $O^{\epsilon1}$	O-1	2.6
				Arg-456 $N^{\eta2}$	O-1	3.0

[a] This salt bridge involves both $N^{\eta1}$ and $N^{\eta2}$ of the respective Arg side chains in each USP.
[b] This pair of salt bridges within the *B. tabaci* ecdysone receptor LBD heterodimeric interface is symmetrically arranged with respect to the heterodimer pseudo 2-fold axis, linking BtEcR-LBD helix H9 to BtUSP-LBD helix H10 on one hand and BtEcR-LBD helix H10 to BtUSP-LBD helix H9 on the other.
[c] The arrangement of the phosphate-coordinating residues suggests that in the absence of the ion an additional salt bridge could be formed by rearrangement of the side chains of BtEcR Arg-384 and BtUSP Glu-387.

actions (42) and may reflect a capacity for the EcR-LBD and USP-LBD to exist as monomers under some circumstances. None of the above differences in the LBD heterodimer interfaces of the *B. tabaci* and *H. virescens* ecdysone receptors can be readily related to the differing bisacylhydrazine affinities of ecdysone receptors from different insect orders.

DISCUSSION

Early *in vitro* studies on the ability of bisacylhydrazine insecticides to compete with tritiated PonA for binding to ecdysone receptors used nuclear extracts from insect cells (10). More recently, similar studies have been performed on EcR-USP heterodimers produced from cloned sequences in rabbit reticulocyte lysates or in extracts from bacterial cells expressing recombinant EcR-USP fusion proteins (37). Such studies have indicated that much of the selective toxicity of these compounds results from their specificity of binding to the different ecdysone receptors. Our studies have taken this approach further to the level of purified ligand-binding regions subcloned from EcR-USP pairs and co-expressed in cultured recombinant insect cells. Our data demonstrate the relevance of studies on purified recombinant ecdysone receptor LBD heterodimers (including the interactions of these simpler proteins with ligands *in vitro*) to whole-insect physiology and development.

Our structural data show that differences in architecture exist between the ligand-binding pocket of the hemipteran ecdysone receptor and its lepidopteran counterpart and that these can tentatively be correlated with the different affinity of receptors from these orders for bisacylhydrazine compounds. We note that BYI06830 contains a relatively large dioxan ring substituent on the bisacylhydrazine B-ring where other bisacylhydrazine compounds carry smaller substituents, and thus it has yet to be established that the observed mode of binding of BYI06830 to HvEcR-LBD is representative of all members of this insecticide family. Nevertheless the involvement of the least conserved region of the ecdysteroid-binding pocket in interactions with BYI06830 is consistent with our suggestion that this region is the source of differential bisacylhydrazine affinity.

Cavities within proteins are a relatively common occurrence and are believed to arise as a compromise imposed by the limits of conformational flexibility *versus* attempts on the part of the protein to achieve close packing (43). They may also reflect regions of the protein that are purposefully less well packed to allow conformational flexibility or dissociation of the surrounding structural elements particularly in domain motions (44). The presence of the ancillary pocket and its structural conservation in both receptors is thus intriguing and may be indicative of flexibility in the protein structure at that location. The structural conservation of this cavity extends further: analogous cavities (Fig. 7) occur in this vicinity in the liver X receptor-β (LXRβ) and in the structure of the farsenoid X-activated receptor (FXR). In the complex of LXRβ-LBD with GW3965 (45), this cavity is occupied by isopropanol, whereas in the complex of LXRβ-LBD with 24(*S*),25-epoxycholesterol (46) the cavity is occupied by water molecules. Single water molecules also occupy volume in this region in the structures of LXRβ-LBD in complex with ligands T-0901317 (47) and A1462 (47). In the structure of FXR-LBD complexed with 6-ethyl-chenodeoxycholic acid (48) and in the structures of LXRβ-LBD in complex with 24(*S*),25-epoxycholesterol (46) the volume corresponding to this cavity extends to the surface of the molecule at a location surrounded by residues from the helix H1/H2 region, the C terminus of helix H5, strand s1, and the N terminus of helix H8. It is reasonable to speculate that if ecdysteroid entry into the EcR-LBD occurs by insertion of the ecdysteroid A-ring into the ligand-binding pocket at a location later capped by helix H12, then the non-planar nature of the ecdysteroid ring system demands flexibility at the base of the pocket as it adjusts to accommodate the ligand. This is a possible reason for the existence of the ancillary cavity. The existence of the cavity may also be related to the observed ability of both the EcR-LBD and LXRβ-LBD to accommodate ligands of stereochemistry quite different than that of the natural ligand, allow-

ing levels of flexibility that might otherwise be precluded. Some of these non-native ligands may also conceivably enter the ligand-binding pocket at the opposite end to that associated with capping by helix H12, perhaps through modes of structural opening such as that seen in the complexed structures of FXR-LBD and LXRβ-LBD mentioned previously. In contrast, the structure of BYI06830-bound HvEcR-LBD shows the ancillary pocket has been "filled in" by structural rearrangements, in particular by the side chains of residues Arg-383 and Tyr-437. Further understanding of the subtleties of packing and of the ligand-induced flexibility in the ecdysone receptor LBD will come from three-dimensional structural data for ecdysone receptors complexed with different ligand chemistries, for example with tetrahydroquinolines (49).

The ability of EcR-LBD to bind ecdysteroids is intimately related to its heterodimerization with USP-LBD (8, 50, 51). It has also been pointed out that the primary sequences of dipteran and lepidopteran USPs are distinct from those of other insect orders (40) with the non-lepidopteran/non-dipteran USPs bearing a closer relationship to mammalian retinoid X receptor proteins than to dipteran or lepidopteran USPs. Because these divisions correlate to some extent with the susceptibility of different insect orders to bisacylhydrazine compounds, this prompted us to compare the heterodimer interface in our hemipteran structure with that in the lepidopteran HvECR-LBD structure in a search for differences that might be associated with differential bisacylhydrazine affinity. However, none of the differences described above have an obvious correlation with bisacylhydrazine affinity, so we look primarily to the EcR component for the basis of the selectivity of this insecticide family.

Tryptophan/histidine activation switches (52) have been proposed for both LXR (46) and FXR (53). The tryptophan residue implicated in these models is equivalent to the residue BtEcR Trp-412, whereas the histidine is replaced by BtEcR Asn-390, an asparagine conserved in all EcR sequences. The perpendicular orientation of the side chains of Trp-412 and Asn-390 in our BtEcR-LBD structure (Fig. 4) suggests an interaction between the π-electron system of Trp-412 and the terminal amino group of Asn-390 that could be further stabilized by interaction of the Asn-390 $O^{\delta 1}$ atom with the hydroxyl group at the C-25 position of the natural ligand 20-hydroxyecdysone. However, such a direct ligand-mediated switch cannot be essential for transactivation as it would not explain why PonA, which lacks a hydroxyl group at C-25, is a very effective agonist.

In conclusion, we have (i) demonstrated that much of the selectivity of the bisacylhydrazine insecticides can be observed at the level of binding to purified recombinant ecdysone receptor LBD heterodimers, (ii) solved the x-ray structure of the first hemipteran ecdysone receptor LBD complexed with an ecdysteroid, and (iii) proposed a tentative explanation for the selectivity of the bisacylhydrazine insecticides, this explanation being derived from differential packing of residues within the walls of the ecdysteroid-binding pockets in EcRs from different taxonomic orders. The silverleaf whitefly ecdysone receptor LBD structure reported in this communication will also be of value in the future design of new hemipteran-selective insecticides.

Acknowledgments—We thank Albert van Donkelaar for assistance with diffraction data collection; Louis Lu for assistance with the baculovirus bioreactor work; and Denis Horn, Mary Alice Yund, and Dinah Hales for stimulating discussions. We thank Colin Ward and Victor Streltsov for valuable comments on the manuscript.

REFERENCES

1. Steinmetz, A. C., Renaud, J. P., and Moras, D. (2001) *Annu. Rev. Biophys. Biomol. Struct.* **30,** 329–359
2. Gronemeyer, H., Gustafsson, J. A., and Laudet, V. (2004) *Nat. Rev. Drug Discov.* **3,** 950–964
3. Enmark, E., and Gustafsson, J. A. (2001) *Trends Pharmacol. Sci.* **22,** 611–615
4. Koelle, M. R., Talbot, W. S., Segraves, W. A., Bender, M. T., Cherbas, P., and Hogness, D. S. (1991) *Cell* **67,** 59–77
5. Oro, A. E., McKeown, M., and Evans, R. M. (1990) *Nature* **347,** 298–301
6. Henrich, V. C., Sliter, T. J., Lubahn, D. B., MacIntyre, A., and Gilbert, L. I. (1990) *Nucleic Acids Res.* **18,** 4143–4148
7. Shea, M. J., King, D. L., Conboy, M. J., Mariani, B. D., and Kafatos, F. C. (1990) *Genes Dev.* **4,** 1128–1140
8. Yao, T. P., Forman, B. M., Jiang, Z., Cherbas, L., Chen, J. D., McKeown, M., Cherbas, P., and Evans, R. M. (1993) *Nature* **366,** 476–479
9. Riddiford, L. M., Cherbas, P., and Truman, J. W. (2000) *Vitam. Horm.* **60,** 1–73
10. Dhadialla, T. S., Carlson, G. R., and Le, D. P. (1998) *Annu. Rev. Entomol.* **43,** 545–569
11. Wing, K. D., Slawecki, R. A., and Carlson, G. R. (1988) *Science* **241,** 470–472
12. Elzen, G. W. (2001) *J. Econ. Entomol.* **94,** 55–59
13. Krust, A., Green, S., Argos, P., Kumar, V., Walter, P., Bornert, J. M., and Chambon, P. (1986) *EMBO J.* **5,** 891–897
14. Evans, R. M. (1988) *Science* **240,** 889–895
15. Renaud, J. P., and Moras, D. (2000) *Cell Mol. Life Sci.* **57,** 1748–1769
16. Billas, I. M., Iwema, T., Garnier, J. M., Mitschler, A., Rochel, N., and Moras, D. (2003) *Nature* **426,** 91–96
17. Clayton, G. M., Peak-Chew, S. Y., Evans, R. M., and Schwabe, J. W. (2001) *Proc. Natl. Acad. Sci. U. S. A.* **98,** 1549–1554
18. Billas, I. M., Moulinier, L., Rochel, N., and Moras, D. (2001) *J. Biol. Chem.* **276,** 7465–7474
19. Hannan, G. N., and Hill, R. J. (1997) *Insect Biochem. Mol. Biol.* **27,** 479–488
20. Hannan, G. N., and Hill, R. J. (2001) *Insect Biochem. Mol. Biol.* **31,** 771–781
21. Cheng, Y., and Prusoff, W. H. (1973) *Biochem. Pharmacol.* **22,** 3099–3108
22. McPherson, A. (1982) *Preparation and Analysis of Protein Crystals*, pp. 96–97, Wiley, New York
23. Otwinowski, Z., and Minor, W. (1996) *Methods Enzymol.* **276,** 307–326
24. Bourguet, W., Vivat, V., Wurtz, J. M., Chambon, P., Gronemeyer, H., and Moras, D. (2000) *Mol. Cell.* **5,** 289–298
25. Vagin, A., and Teplyakov, A. (1997) *J. Appl. Crystallogr.* **30,** 1022–1025
26. Collaborative Computing Project No. 4 (1994) *Acta Crystallogr. Sect. D Biol. Crystallogr.* **50,** 760–763
27. Brünger, A. T., Adams, P. D., Clore, G. M., DeLano, W. L., Gros, P., Grosse-Kunstleve, R. W., Jiang, J. S., Kuszewski, J., Nilges, M., Pannu, N. S., Read, R. J., Rice, L. M., Simonson, T., and Warren, G. L. (1998) *Acta Crystallogr. Sect. D* **54,** 905–921
28. Jones, T. A., Zou, J. Y., Cowan, S. W., and Kjeldgaard, M. (1991) *Acta Crystallogr. Sect. A* **47,** 110–119
29. Laskowski, R. A., MacArthur, M. W., Moss, D. S., and Thornton, J. M. (1993) *J. Appl. Crystallogr.* **26,** 283–291
30. Kleywegt, G. J. (1994) *Acta Crystallogr. Sect. D Biol. Crystallogr.* **50,** 178–185
31. Jones, T. A., Zou, J. Y., Cowan, S. W., and Kjeldgaard, M. (1991) *Acta Crystallogr. Sect. A* **47,** 110–119
32. Hubbard, S. J., and Argos, P. (1995) *Protein Eng.* **8,** 1011–1015
33. Connolly, M. L. (1983) *Science* **221,** 709–713
34. McDonald, I. K., and Thornton, J. M. (1994) *J. Mol. Biol.* **238,** 777–793
35. Brünger, A. T. (1992) *Nature* **355,** 472–474
36. Wurtz, J. M., Bourguet, W., Renaud, J. P., Vivat, V., Chambon, P., Moras, D., and Gronemeyer, H. (1996) *Nat. Struct. Biol.* **3,** 87–94
37. Smagghe, G., Dhadialla, T. S., and Lezzi, M. (2002) *Insect Biochem. Mol. Biol.* **32,** 187–192
38. Yund, M. A., King, D. S., and Fristrom, J. W. (1978) *Proc. Natl. Acad. Sci. U. S. A.* **75,** 6039–6043
39. Harmatha, J., and Dinan, L. (1997) *Arch. Insect Biochem. Physiol.* **35,** 219–225
40. Bonneton, F., Zelus, D., Iwema, T., Robinson-Rechavi, M., and Laudet, V. (2003) *Mol. Biol. Evol.* **20,** 541–553
41. Egea, P. F., Mitschler, A., and Moras, D. (2002) *Mol. Endocrinol.* **16,** 987–997
42. Bahadur, R. P., Chakrabarti, P., Rodier, F., and Janin, J. (2004) *J. Mol. Biol.* **336,** 943–955
43. Hubbard, S. J., Gross, K. H., and Argos, P. (1994) *Protein Eng.* **7,** 613–666
44. Hubbard, S. J., and Argos, P. (1996) *J. Mol. Biol.* **261,** 289–300
45. Färnegardh, M., Bonn, T., Sun, S., Ljunggren, J., Ahola, H., Wilhelmsson, A., Gustafsson, J. A., and Carlquist, M. (2003) *J. Biol. Chem.* **278,** 38821–38828
46. Williams, S., Bledsoe, R. K., Collins, J. L., Boggs, S., Lambert, M. H., Miller, A. B., Moore, J., McKee, D. D., Moore, L., Nichols, J., Parks, D., Watson, M., Wisely, B., and Willson, T. M. (2003) *J. Biol. Chem.* **278,** 27138–27143
47. Hoerer, S., Schmid, A., Heckel, A., Budzinski, R. M., and Nar, H. (2003) *J. Mol. Biol.* **334,** 853–861
48. Downes, M., Verdecia, M. A., Roecker, A. J., Hughes, R., Hogenesch, J. B., Kast-Woelbern, H. R., Bowman, M. E., Ferrer, J. L., Anisfeld, A. M., Edwards, P. A., Rosenfeld, J. M., Alvarez, J. G., Noel, J. P., Nicolaou, K. C., and Evans, R. M. (2003) *Mol. Cell* **11,** 1079–1092
49. Kumar, M. B., Potter, D. W., Hormann, R. E., Edwards, A., Tice, C. M., Smith, H. C., Dipietro, M. A., Polley, M., Lawless, M., Wolohan, P. R., Kethidi, D. R., and Palli, S. R. (2004) *J. Biol. Chem.* **279,** 27211–27218
50. Bergman, T., Henrich, V. C., Schlattner, U., and Lezzi, M. (2004) *Biochem. J.* **378,** 779–784
51. Lezzi, M., Bergman, T., Henrich, V. C., Vogtli, M., Fromel, C., Grebe, M., Przibilla, S., and Spindler-Barth, M. (2002) *Eur. J. Biochem.* **269,** 3237–3245
52. Ma, J. C., and Dougherty, D. A. (1997) *Chem. Rev.* **97,** 1303–1324
53. Mi, L. Z., Devarakonda, S., Harp, J. M., Han, Q., Pellicciari, R., Willson, T. M., Khorasanizadeh, S., and Rastinejad, F. (2003) *Mol. Cell* **11,** 1093–1100
54. Kraulis, P. J. (1991) *J. Appl. Crystallogr.* **24,** 946–950
55. Lawrence, M. C., and Bourke, P. (2000) *J. Appl. Crystallogr.* **33,** 990–991
56. Merritt, E. A., and Bacon, D. J. (1997) *Methods Enzymol.* **277,** 505–524
57. Thompson, J. D., Higgins, D. G., and Gibson, T. J. (1994) *Nucleic Acids Res.* **22,** 4673–4680
58. Barton, G. J. (1993) *Protein Eng.* **6,** 37–40